

Direct elementary reactions of boron and nitrogen at high pressures and temperatures

C. S. Yoo,* J. Akella, and H. Cynn

Lawrence Livermore National Laboratory, Livermore, California 94551

M. Nicol

University of California, Los Angeles, Los Angeles, California 90095

(Received 17 October 1996; revised manuscript received 9 January 1997)

Highly exothermic direct reactions between elements boron and nitrogen at high pressures and temperatures yield technologically important forms of hexagonal and cubic boron nitride (BN). The crystal structures of the reaction products vary with pressure. Below 10 GPa, hexagonal BN is the product; cubic or wurzite BN form at higher pressures. Under nitrogen-rich conditions, another hexagonal allotrope occurs; this seems to be a highly transparent, low density h' -BN. No direct reactions occur at ambient temperature even at pressures as high as 50 GPa, implying that a large activation barrier limits the kinetics of these exothermic processes. Direct reactions between boron and oxygen are also discussed. [S0163-1829(97)01825-0]

I. INTRODUCTION

Many important materials composed of first- and second-row elements like diamond and cubic boron nitride, c -BN, have covalently bonded three-dimensional network structures. The extended networks of these hard materials contrast with the molecular forms of the same elements like N_2 with strong covalent intramolecular bonds and weak van der Waals interactions between the molecules. The highly local nature of the electrons in these molecular covalent bonds minimizes their potential energy, makes the bonds extremely stable, and acts as a barrier to reactions leading to network structures.

Applying pressure is, however, inimical to covalent bonds. The kinetic and potential energies of electrons vary with density as $\rho^{2/3}$ and $\rho^{1/3}$, respectively, and the kinetic energy should dominate at high densities. Electrons in local covalent bonds, therefore, eventually delocalize at high densities, converting molecular materials to more closely packed network structures and to metals at high pressures. Many experiments in covalent molecular systems support such a principle. Most unsaturated organic molecules including CO and C_2N_2 polymerize at pressures of the order of 10 GPa.^{1,2} Layered covalent solids like graphite and h -BN transform to dense, three-dimensional network materials, diamond and c -BN, at high pressures.³⁻⁵ A covalently bonded network structure has also been suggested for β - C_3N_4 , proposed as a superhard material.^{6,7} Many diatomic molecules, halogen, and inert gases even metallize at the pressures of 100 GPa.⁸⁻¹²

While applying pressure modifies the thermodynamic reactivity of covalent molecules, large activation barriers often limit reaction rates at high pressures. For example, a recent theoretical study shows that nitrogen polymerizes to a three-dimensional network structure analogous to phosphorous at 60 GPa.¹³ However, no nitrogen polymer has been detected in experiments at pressures as high as 130 GPa,¹⁴ presumably because of large kinetic barriers. The graphite-to-diamond transformation strongly depends on nucleation and growth kinetics; and, at any pressure, diamond has only been

synthesized under kinetic control or at substantially higher than the equilibrium transition temperature.¹⁵⁻¹⁷ Recently developed diamond-anvil cell (DAC) laser-heating techniques provide a way to overcome activation barriers at high pressures.¹⁸⁻²²

In this study, we combined DAC laser-heating and synchrotron x-ray diffraction methods for *in-situ* material synthesis and characterization at high temperatures and pressures. We report the observation of the direct reactions of nitrogen with boron yielding three forms of boron nitride: c -BN, h -BN, and what we believe is a second hexagonal form, h' -BN. Observations during experiments with boron and oxygen are also described to show the generality of this method.

II. EXPERIMENTS

The experiments were done with a modified Merrill-Bassett cell.²³ A maraging steel seat with a slit for easy optical access and restricted x-ray transmission backed one diamond, while a beryllium seat with low x-ray absorption backed the other diamond. Boron powder and a few pieces of ruby dust for pressure measurements were loaded into the 150- μ m sample hole in a spring steel or rhenium gasket. Nitrogen or oxygen was then added by an immersion technique.

The samples were heated by a cw Nd:YAG laser micro-focussed along an axis about 30° from the normal to the diamond culets. A chromatically corrected objective ($\times 20$, Leitz) collected thermal emission from the sample along an axis about 15° from the normal (and 45° from the laser axis). A 75- μ m pinhole limited the field of view of the collection optics to the central 4 μ m of the heated area. A single-core 200 μ m fiber delivered the thermal emission from the pinhole to a spectrometer with a cooled charge-coupled device (CCD) detector. Temperatures were determined by fitting the thermal emission spectrum to a gray-body expression.

Angle-resolved x-ray diffraction patterns of laser-heated

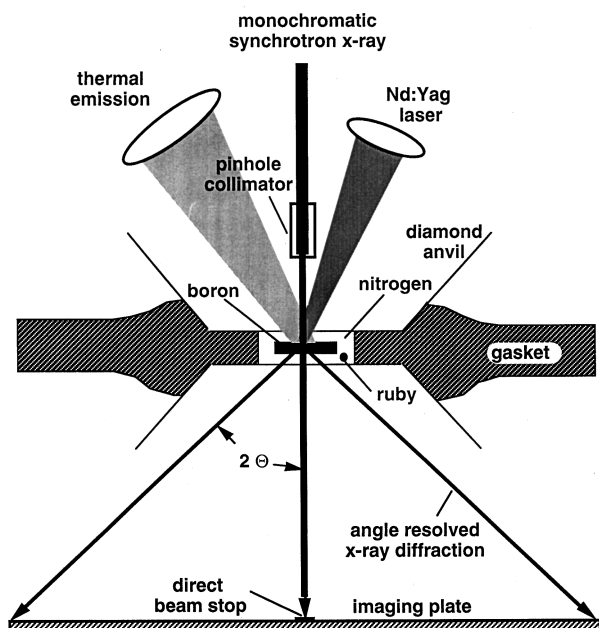


FIG. 1. An experimental setup for angle-resolved x-ray diffraction measurements of the laser-heated samples in a diamond-anvil cell. The system is capable of synthesis and *in-situ* characterization of material at high pressures and temperatures.

samples and products were obtained *in situ* at high pressures and temperatures using the system shown in Fig. 1.²⁴ We focused 20-keV x-ray, diffracted from the Si(220) double-crystal monochromator, to intersect the sample at the focus of the laser-heating system. A 20-by-40 cm image plate,

typically separated from the sample by 20 cm, collected the diffraction patterns. Diffraction features with 2 to 26° register along all directions on the plate, while features up to 45° can be detected along the long dimension. Images were read with a Fuji BAS2000 scanner at 100 μm resolution.

A 60- μm Pt pinhole collimator about 5 cm before the sample limits the diameter of the x-ray beam. Nevertheless, the beam remains slightly larger than the hot spot, whose diameter is 30-to-50 μm depending upon the temperature. Thus, the diffraction patterns originate over the full, relatively large range of temperatures. Temperatures discussed here, therefore, should be considered only as the upper limit for the hottest spot of the sample and should not be overinterpreted. High transient temperature excursions during the rapid stages of these highly exothermic reactions make precise characterization of the sample temperatures even less realistic.

III. RESULTS

Figure 2 illustrates highly exothermic nature of direct elementary reactions between boron and oxygen at 6.9 GPa; boron-nitrogen reactions occur qualitatively the same way. Boron powders were prepressed to the shape, about 10 μm in thickness, between diamond anvils prior to the loading in liquid O_2 . Before heating (a), the boron sample appears opaque in the nearly transparent oxygen. Boron strongly absorbs infrared radiation so the sample temperature can easily be increased in small steps by adjusting the power of the Nd:YAG output at 1.06 μm , as shown in frames (b) through (e). Above 1300 K, the thermal emission from the hot areas became very obvious; however, the sample did not change

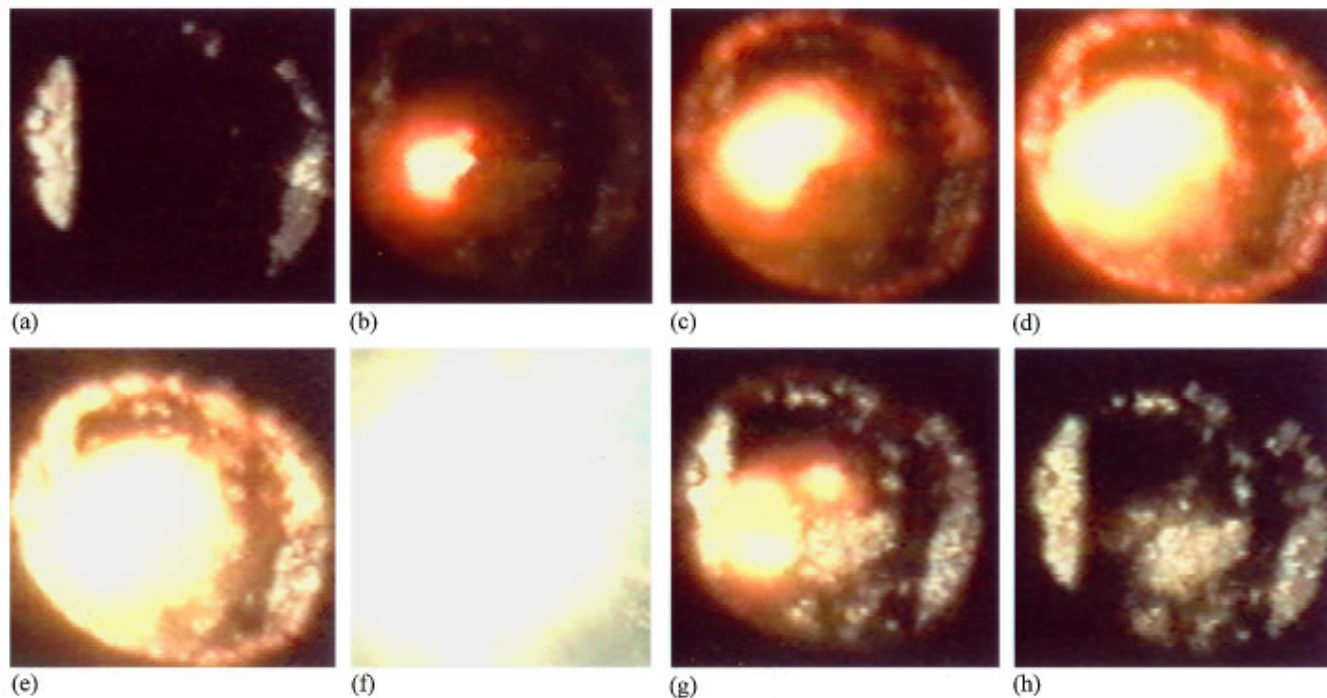


FIG. 2. (Color) Images captured from videotape records of a boron-oxygen sample during the laser heating experiment at 6.9 GPa: (a) before heating, (b)–(e) during heating prior to the reaction, (f) at the onset of reaction, (g) after the reaction, and (h) after heating. These images show that the reaction is highly exothermic, resulting in a highly transparent product. The direct reactions between boron and nitrogen appear qualitatively the same way.

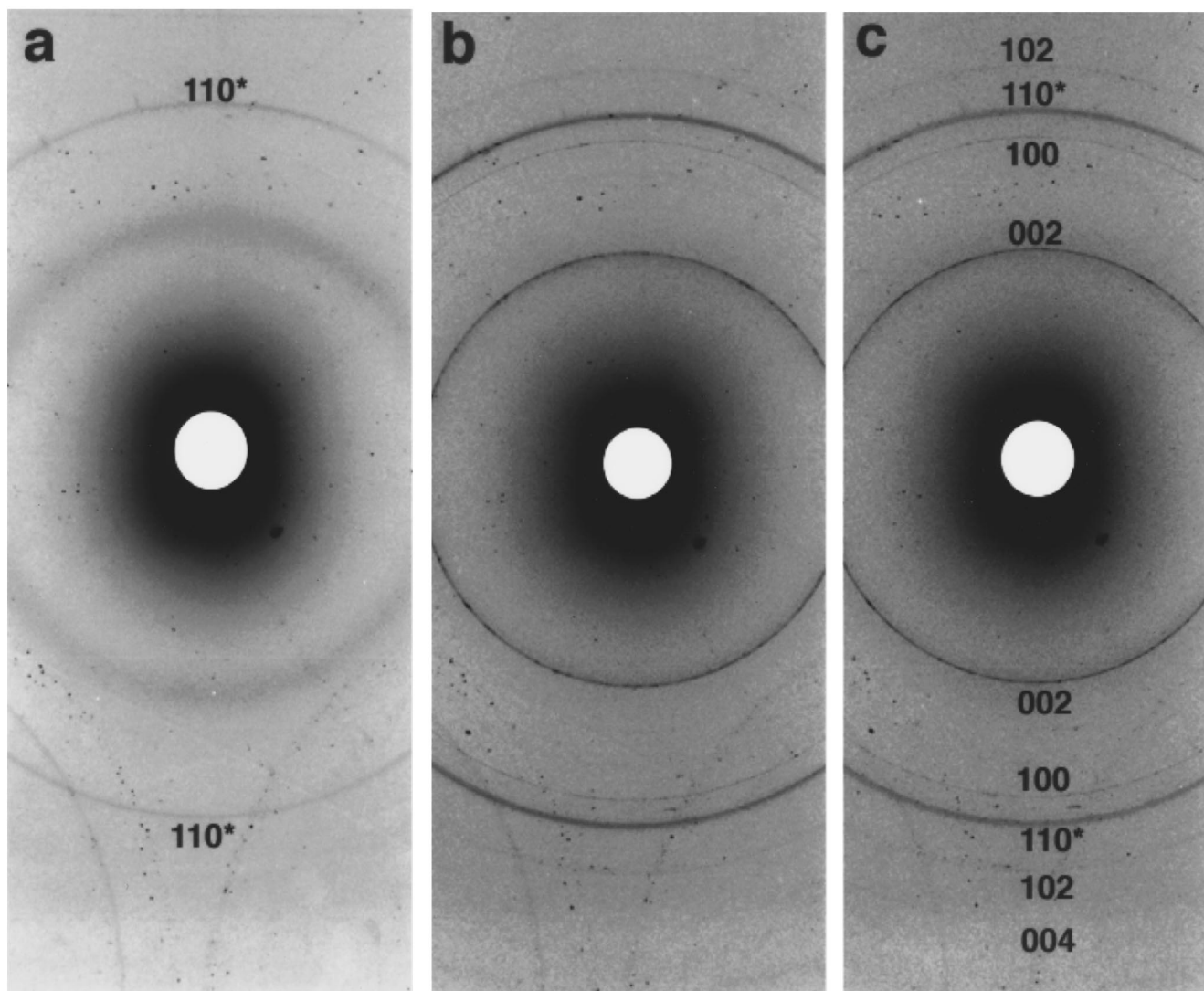


FIG. 3. Angle-resolved x-ray diffraction patterns of the boron-nitrogen mixture obtained (a) before, (b) during, and (c) after the laser-heating at 2 GPa. Each diffraction patterns were recorded to $2\Theta = 45^\circ$ on an imaging plate detector. The results clearly indicate *h*-BN forms as a result of the direct reaction of elements boron and nitrogen. The indexing in (c) was for *h*-BN (Table I); the (110) reflection with an asterisk was from the gasket.

appearance at these temperatures. At higher laser powers and temperatures, the intensity of the thermal emission abruptly increases as is evident from the flashes of light (f). After combustion (g), the intensity of the emission dropped rapidly; and the sample lost luminosity even for higher laser powers because very transparent products formed (h) which were recovered at ambient temperature and pressure. These elementary reactions of boron with oxygen and nitrogen yield highly transparent and well crystallized products, in contrast to other synthetic methods using catalytic and/or nucleation materials and typically resulting in highly colored and low crystallized products. The threshold temperatures for boron reacting with nitrogen and oxygen and approximately 1800 and 2300 K, respectively. The peak temperatures achieved during reaction were not measured.

Figure 3 shows angle-resolved x-ray diffraction patterns of boron-nitrogen samples (a) before, (b) during, and (c) after heating at 2 GPa. The reaction temperature of (b) was about 1800 K. We attribute the very diffuse features in (a),

corresponding to *d* spacings of about 3.0 and 2.0 Å, to amorphous boron and/or fluid nitrogen and the (110) reflection of α (bcc)-Fe from the edge of a spring steel gasket. During heating, this diffuse feature substantially weakens or disappears (b); and several new sharp diffraction rings arise, including strong features at 3.33 and 2.17 Å and several weaker rings at smaller *d* spacings. All of the new rings remain after heating (c), clearly indicating that the sample changed irreversibly. The transparent appearance of the quenched product also indicates that a chemical reaction occurs at high temperatures.

The diffraction patterns in Figs. 3(b) and 3(c) are readily indexed in terms of hexagonal *h*-BN, as shown in Table I. This indexing yields densities and lattice parameters nearly identical to literature values for this material.²⁵ The sharpness and relative intensity of the rings in this pattern indicate the *h*-BN product is highly crystalline, in contrast to the highly distorted *h*-BN (that is, turbostratic *t*-BN) produced by other chemical methods.^{26–30} In fact, all *h*-BN synthesized in

TABLE I. X-ray diffraction patterns of *h*-BN and *h'*-BN at ambient condition, synthesized from the direct elementary reactions of boron and nitrogen at high pressures and temperatures.

<i>h</i> -BN* ^a				<i>h'</i> -BN* ^b			
(<i>hkl</i>)	<i>d</i> _{cal} (Å)	<i>d</i> _{obs} (Å)	Δ <i>d</i> (Å)	(<i>hkl</i>)	<i>d</i> _{cal} (Å)	<i>d</i> _{obs} (Å)	Δ <i>d</i> (Å)
002	3.342	3.341	0.001	100	2.854	2.854	0.000
100	2.186	2.186	0.000	002	2.529	2.527	0.002
102	1.830	1.830	0.000	102	1.892	1.892	0.000
004	1.671	1.672	0.001	110	1.647	1.643	0.004
104	1.328	1.332	0.004	200	1.426	1.428	0.002
110	1.262	1.263	0.001	112	1.380	1.385	0.005
112	1.181	1.179	0.002	201	1.242	1.242	0.000
114	1.007			104	1.157	1.157	0.000
<i>a=b</i>	2.524±0.020 Å		2.504 Å* ^c	<i>a=b</i>	3.295±0.002 Å		
<i>c</i>	6.684±0.020 Å		6.661 Å* ^c	<i>c</i>	5.055±0.020 Å		
<i>c/a</i>	2.648		2.660* ^c	<i>c/a</i>	1.534		
<i>V</i>	0.4474 cm ³ /g			<i>V</i>	0.5767 cm ³ /g		

^aThe *h*-BN sample was quenched from approximately 1800 K at 2.0 GPa, shown in Fig. 3(c).

^bThe *h'*-BN sample was quenched from approximately 1300 K at 2.0 GPa, shown in the lower trace of Fig. 4.

^cAfter R. S. Pease, Acta Crystallogr. **5**, 356 (1952).

the present study had similarly high crystallinity. It may, therefore, be possible to obtain a highly pure single phase of *h*-BN and to control the crystallinity at high pressures.

The crystal structure of final BN products changes with pressure. Above 10 GPa, the direct reaction yields cubic *c*-BN. Table II summarizes the diffraction pattern of the BN product at 14.6 GPa and room temperature quenched from about 2300 K. Major diffraction features of the pattern were well indexed in terms of *c*-BN and cubic δ -N₂. Based on these assignments, the density of *c*-BN is 3.596 g/cm³, very consistent with the measured equation of state of *c*-BN at 14.6 GPa, 3.614 g/cm³.³¹ The difference less than 0.5% in

density is probably due to distortions introduced during quenching. The lattice parameter of δ -N₂, *a*=5.692 Å (*V*=13.884 cm³/mol), is also very consistent with the reported value extrapolated to the same pressure, 5.699 Å (13.936 cm³/mol).^{32,33} The peak at 2.23 Å probably is the (100) reflection of wurzite *w*-BN; the (100) of *w*-BN was at 2.21 Å in previous studies.^{34,35} Other minor features at 1.98 and 1.14 Å probably are the (101) and (200) reflections of *w*-BN, which might overlap with the (101) and (211) reflections of α -Fe from the gasket. Weak diffused features at 2.23 and 1.88 Å have not been indexed.

The chemical compositions of the initial mixtures seem to

TABLE II. The crystal structure of *c*-BN synthesized directly from its elements at 14.6 GPa and about 2300 K. The diffraction was obtained at 14.6 GPa and room temperature.

<i>M</i> (<i>h,k,l</i>)	<i>d</i> _{obs}	<i>I</i> _{obs} * ^a	<i>d</i> _{cal}	<i>I</i> _{cal} * ^b	Δ <i>d</i>
δ -N ₂ (200)	2.8460	25	2.8460	89	0.0000
δ -N ₂ (210)	2.5440	75	2.5455	100	0.0015
δ -N ₂ (211)	2.3232	57	2.3237	91	0.0005
<i>w</i> -BN(100)	2.2306	28			
	2.1382	33			
<i>c</i> -BN(111) <i>w</i> -BN(002)	2.0659	100	2.0660	100	0.0001
<i>w</i> -BN(101) α -Fe(101)	1.9780	62			
<i>c</i> -BN(200)	1.7980	46	1.7890	8	0.0090
	1.7809	51			
<i>c</i> -BN(220) <i>w</i> -BN(110)	1.2654	49	1.2650	33	0.0004
<i>w</i> -BN(200) α -Fe(211)	1.1446	15			
<i>c</i> -BN(311)	1.0796	13	1.0790	20	0.0006

δ -N₂: *a*=5.6920 Å

c-BN: *a*=3.5782 Å, *V*=0.2781 cm³/g, ρ =3.5958 g/cm³ (cf. ρ =3.4678 g/cm³ at 1 atm)

^aThe intensity is in arbitrary units, normalized to the intensity of the *c*-BN(111) reflection.

^bThe calculated intensity for *c*-BN and δ -N₂ are normalized to the (111) reflection for *c*-BN and the (210) for δ -N₂.

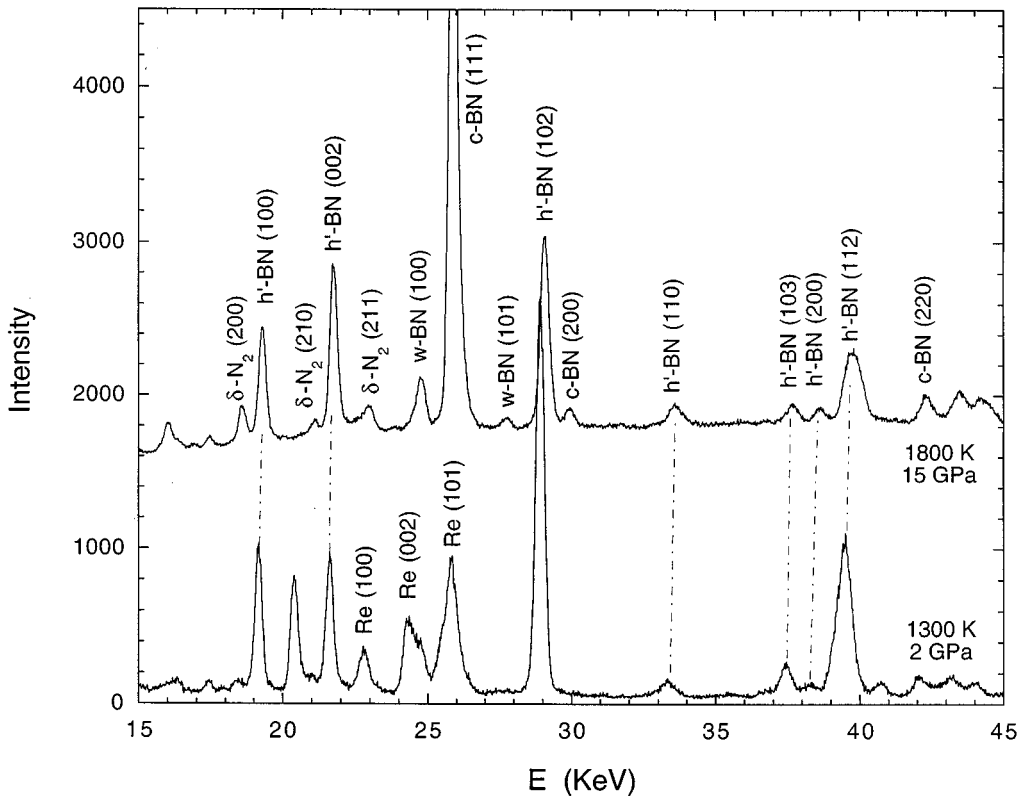


FIG. 4. Energy-dispersive x-ray diffraction patterns of the boron-nitrogen reaction products in nitrogen-rich conditions at 15 GPa quenched from 1800 K (upper pattern) and at 2 GPa quenched from 1300 K (lower pattern). The indexings for *w*-BN and *c*-BN in the upper trace are consistent with those synthesized in a boron-rich condition shown in Table II. The indexing for *h'*-BN is listed in Table I. These data were obtained at $E_d = 54.754 \text{ keV } \text{\AA}$.

influence the crystal structure of the final products. Figure 4 shows the energy-dispersive x-ray diffraction patterns of laser-heated nitrogen-rich mixtures (upper trace) at 15 GPa after quenching from 1800 K and (lower trace) at 2 GPa after quenching from 1300 K. Features at 25.84, 29.96, and 42.32 keV in Fig. 5(a) match closely to the (111), (200), and (220) diffraction patterns of *c*-BN; and the bands at 24.76, 25.89, and 27.80 keV match the (100), (002), and (101) patterns of *w*-BN.^{34,35} The computed densities of *c*-BN and *w*-BN at 15 GPa are 3.458 and 3.480 g/cm³, respectively. These values are approximately consistent with those at ambient conditions, 3.487 and 3.490 g/cm³, respectively. On the other hand, the compression of *c*-BN is smaller by 4.3% than the previously reported value at 15 GPa,³¹ probably due to large distortions introduced by coexistence of other phases such as *w*-BN and one described below.

Other series of diffraction features appear in Fig. 4(a). The relatively weak features at 18.60, 21.11, and 22.99 keV are indexed as three strong reflections of δ -N₂, (200), (210), and (211).^{32,33} We index seven other features as parts of the diffraction pattern of a hexagonal structure, probably a boron nitride, which we designate as *h'*-BN to distinguish it from the familiar *h*-BN. The unit cell volume of *h'*-BN is substantially larger than that of *h*-BN; see Table I. Features attributed to *h'*-BN also appear in patterns of products obtained at lower pressures like that in Fig. 4(b). Three broad features in that pattern arise from the rhenium gasket, but the 20.5-keV feature could not be satisfactorily indexed. Nitrogen is fluid at this pressure and, thus, yields no sharp diffraction lines.

The reactions to *h'*-BN seem to occur only in N₂-rich

conditions. For example, in many other cases when large amounts of boron powder were used, the reaction typically produced either nearly pure *h*-BN at low pressures (Fig. 3) or *c*-BN above 10 GPa (Table II). *h'*-BN is highly transparent and can be recovered as white polycrystals at ambient pressure. Figure 5 compares scanning electron micrographs of *h'*-BN and *h*-BN recovered from 1300 K and 2.0 GPa and 1800 K and 1.9 GPa, respectively. Both samples have plate-like structures, typical of layered hexagonal materials. However, *h'*-BN has many microholes which may be the escaped routes for excess nitrogen in the sample or captured in the BN lattice. We have not seen *h'*-BN converting to other forms of boron nitride at ambient condition, although it appears to be unstable when exposed to high power lasers.

IV. DISCUSSION

The very exothermic nature of the boron-nitrogen reaction is typical for many elementary reactions of first- and second-row elements leading to oxides, nitrides, and carbides. Reactions resulting in various oxides and nitrides are highly exothermic, whereas those yielding hydrides and nitrogen polymer¹³ demand the most energy. Despite the thermodynamic stability of boron nitride at high pressures, boron and nitrogen do not react at ambient temperature even at 50 GPa, the highest pressure of our experiments. This observation implies that there is a large kinetic barrier to reaction, especially in the dissociation of N₂.

Pressure-volume considerations also favor the forward boron-nitrogen reaction. At 2 GPa, the molar volume, 10.58

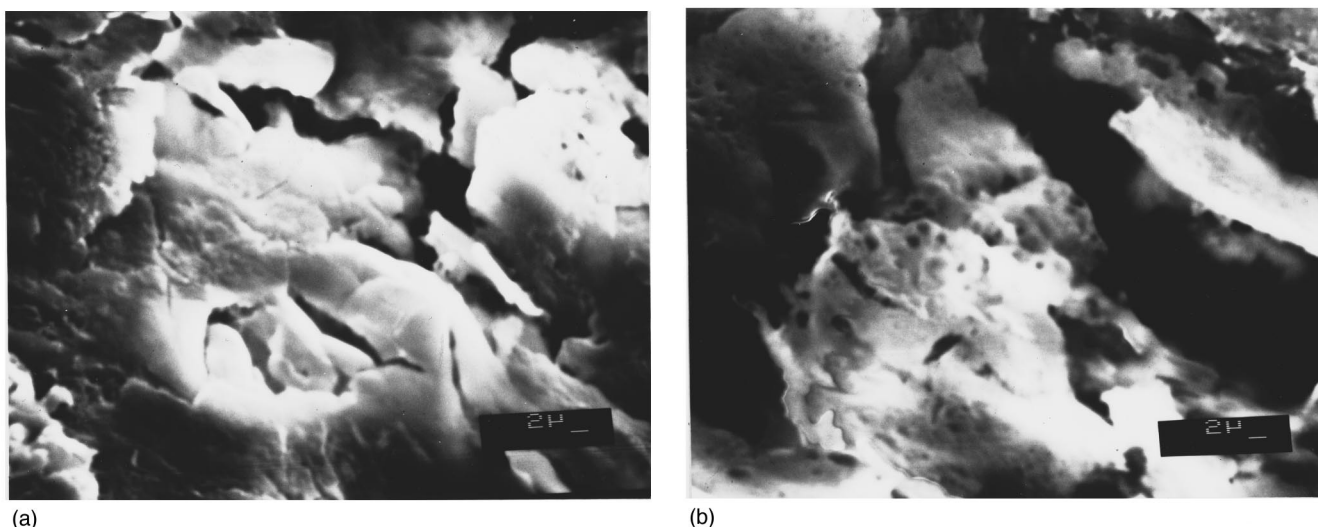


FIG. 5. Scanning electron microscope images of two hexagonal allotropes of boron nitride for comparison: (a) *h*-BN and (b) *h'*-BN. Both materials form layered flakes. We attribute the holes in *h'*-BN to evaporation of excess nitrogen.

cm^3/mol , of *h*-BN (Ref. 36) is nearly 38% less than the volume of a mole of boron, $4.57 \text{ cm}^3/\text{mol}$,³⁷ and one-half mole of N_2 , $10.03 \text{ cm}^3/\text{mol}$.^{32,33} Although this difference decreases to about 30% at 6 GPa and 22% at 10 GPa, the density change alone favors production of *h*-BN to 10 GPa. At higher pressures, denser *c*-BN (Ref. 31) is the product, and the density difference from the mixture of the elements is even larger. At 10 GPa, *c*-BN, $6.93 \text{ cm}^3/\text{mol}$, is 42% denser than *h*-BN, $9.82 \text{ cm}^3/\text{mol}$.

The crystal structure of the BN reaction products is dictated by its thermodynamic stability at high pressures. Samples with comparable initial amounts of boron and nitrogen yielded only *h*-BN below 7.5 GPa, while *c*-BN was the unique product above 10 GPa, approximately consistent with their reported stability fields.¹⁵⁻¹⁷ However, this transition pressure of boron-nitrogen reaction, 7–10 GPa, appears to be somewhat higher than the previously reported hexagonal-to-cubic phase transition pressure, 5–7 GPa at 2000 K.^{15,34,38-40} This difference perhaps represents the kinetic effects of the reaction. No diffraction lines of low-pressure BN phases, rhombohedral *r*-BN or *h*-BN, occur in Table II and Fig. 4(a). Neither *c*-BN nor *w*-BN is produced together with *h*-BN at low pressures as seen in Fig. 3. These observations are inconsistent with the hypothesis that the direct reaction between boron and nitrogen leading to *c*-BN at high pressures proceeds through an *h*-BN intermediate. Instead, at high pressures and temperatures, *c*-BN forms directly by a reaction between elemental boron and nitrogen. *c*-BN has typically been synthesized from *h*-BN at high *P*, *T* conditions,^{15,16,34} and we believe that this shows *c*-BN directly synthesized from its elements.

The *h'*-BN phase is probably a nitrogen-rich metastable

form of B_xN_y . This conjecture stems from the fact that *h'*-BN occurs only in nitrogen-rich conditions regardless the stability fields of *h*-BN and *c*-BN. The low density (Table I) and morphology (Fig. 5) of this phase also support such a hypothesis. Clearly, further studies are needed to determine the exact nature of crystal structure, stoichiometry, and stability of *h'*-BN.

In summary, we have shown a synthetic route for *c*-BN and *h*-BN directly from its elements at high pressures and temperatures. A similar concept of boron-nitrogen reactions can be applicable for synthesis of other technologically important materials made of first and second row elements.⁴¹ Furthermore, since the crystal structures of direct reaction products depend largely on pressure, it may be feasible to engineer the final product based on its thermodynamic stability at various pressure-temperature conditions.

ACKNOWLEDGMENTS

The angle-resolved x-ray measurements were done at the University of California-National Laboratories PRT Beam Line at the Stanford Synchrotron Radiation Laboratory. The energy-dispersive x-ray measurements were made at the National Synchrotron Light Source. We thank C. Ruddle of LLNL for assisting with the experiments, B. Goodwin, C. Mailhot, N. Holmes for supporting this study, and M. Ross and D. Young for valuable discussions of the results. This work was performed under the auspices of the U.S. Department of Energy Contract No. W-7405-ENG-48 at Lawrence Livermore National Laboratory, NSF Grant No. DMR 94-12187, and a grant from the Livermore Branch of the University of California IGPP.

* Author to whom correspondence should be addressed.

¹C. S. Yoo and M. F. Nicol, *J. Phys. Chem.* **90**, 6726 (1986); **90**, 6732 (1986); C. S. Yoo, Ph.D. thesis, UCLA, 1986.

²A. I. Katz, D. Schiferl, and R. L. Mills, *J. Phys. Chem.* **88**, 3176 (1981).

³Q. Johnson and A. C. Mitchell, *Phys. Rev. Lett.* **29**, 1369 (1972).

⁴J. R. Riter, Jr., *J. Chem. Phys.* **59**, 1538 (1973).

⁵F. P. Bundy, *J. Geophys. Res.* **85**, 6930 (1980).

⁶A. Y. Liu and M. L. Cohen, *Science* **245**, 841 (1989).

⁷D. M. Tarter and R. J. Hemley, *Science* **271**, 53 (1996).

⁸K. A. Goettel, J. H. Eggert, and I. F. Silvera, *Phys. Rev. Lett.* **62**, 665 (1989).

- ⁹R. Reichlin, M. Ross, S. Martin, and K. A. Goettel, *Phys. Rev. Lett.* **56**, 2858 (1986).
- ¹⁰S. T. Weir, A. C. Mitchell, and W. J. Nellis, *Phys. Rev. Lett.* **76**, 1860 (1996).
- ¹¹R. J. Hemley and H. K. Mao, *Science* **249**, 391 (1990).
- ¹²H. E. Lorenzana, I. F. Silvera, and K. A. Goettel, *Phys. Rev. Lett.* **65**, 1901 (1990).
- ¹³C. Mailhiot, L. H. Yang, and A. K. McMahan, *Phys. Rev. B* **46**, 14 419 (1992).
- ¹⁴R. Reichlin, D. Schiferl, S. Martin, C. Vanderborgh, and R. L. Mills, *Phys. Rev. Lett.* **55**, 1464 (1985).
- ¹⁵F. R. Corrigan and F. P. Bundy, *J. Chem. Phys.* **63**, 3812 (1975).
- ¹⁶F. P. Bundy and J. S. Kasper, *J. Chem. Phys.* **46**, 3437 (1967); F. P. Bundy, *Physica A* **156**, 169 (1989).
- ¹⁷M. van Thiel and F. H. Ree, *Phys. Rev. B* **48**, 3591 (1993); *Int. J. Thermophys.* **10**, 227 (1989).
- ¹⁸L. C. Ming and W. Bassett, *Rev. Sci. Instrum.* **45**, 1115 (1974).
- ¹⁹S. K. Saxena, G. Shen, and P. Lazor, *Science* **260**, 1312 (1993).
- ²⁰A. Zerr and R. Boehler, *Science* **262**, 553 (1993).
- ²¹D. L. Heinz and R. Jeanloz, *J. Geophys. Res.* **92**, 11 437 (1987).
- ²²C. S. Yoo, J. Akella, A. J. Campbell, H. K. Mao, and R. J. Hemley, *Science* **270**, 1473 (1995).
- ²³L. Merrill and W. A. Bassett, *Rev. Sci. Instrum.* **45**, 290 (1974).
- ²⁴Angle-resolved x-ray diffraction patterns at high pressures and temperatures were obtained at the Stanford Synchrotron Radiation Laboratory (SSRL), and patterns of quenched samples were collected at the National Synchrotron Light Source (NSLS) by energy dispersive methods [J. Hu, H.-K. Mao, J. Shu, and R. J. Hemley, in *High Pressure Science and Technology-1993*, edited by S. C. Schmidt, J. W. Shanner, G. A. Samara, and M. Ross (AIP Press, New York, 1994), Part 1, p. 441].
- ²⁵R. S. Pease, *Acta Crystallogr.* **5**, 356 (1952).
- ²⁶T. Sekine and T. Sato, *J. Appl. Phys.* **74**, 2440 (1993).
- ²⁷S. Horiuchi, L.-L. He, and M. Akaishi, *Appl. Phys. Lett.* **68**, 182 (1996).
- ²⁸S. Komatsu, Y. Moriyoshi, M. Kasamatsu, and K. Yamada, *J. Appl. Phys.* **70**, 7078 (1991).
- ²⁹B. Wiley and R. Kaner, *Science* **255**, 1093 (1996).
- ³⁰E. G. Gilan and R. B. Kaner, *Chem. Mater.* **8**, 333 (1996).
- ³¹E. Knittle, R. M. Wentzcovitch, R. Jeanloz, and M. L. Cohen, *Nature (London)* **337**, 349 (1989).
- ³²D. T. Cromer, R. L. Mills, D. Schiferl, and L. A. Schwalbe, *Acta Crystallogr. Sec. B* **37**, 8 (1981).
- ³³B. Olinger, *J. Chem. Phys.* **80**, 1309 (1984).
- ³⁴F. P. Bundy and R. H. Wentoff, Jr., *J. Chem. Phys.* **38**, 1144 (1963).
- ³⁵T. Soma, A. Sawaoka, and S. Saito, *Mater. Res. Bull.* **9**, 755 (1974).
- ³⁶R. W. Lynch and H. G. Drickamer, *J. Chem. Phys.* **44**, 181 (1966).
- ³⁷R. J. Nelmes, J. S. Loveday, D. R. Allan, J. M. Besson, G. Hamel, P. Grima, and S. Hull, *Phys. Rev. B* **47**, 7668 (1993).
- ³⁸S. Nakano and O. Fukunaga, *Diam. Relat. Mater.* **2**, 1409 (1993).
- ³⁹M. Ueno, K. Hasegawa, R. Oshima, A. Onodera, O. Shinomura, K. Takemura, H. Nakae, T. Matsuda, and T. Hirai, *Phys. Rev. B* **45**, 10 226 (1992).
- ⁴⁰V. L. Solozhenko, *Diam. Relat. Mater.* **4**, 1 (1994).
- ⁴¹C. S. Yoo, J. Akella, and M. F. Nicol, in *Advanced Materials '96*, edited by M. Kamo, H. Kanda, Y. Matsui, and T. Sekine (Intl. Commun. Spec., Tokyo, 1996), p. 175.